



National Defence
Research and
Development Branch

Défense nationale
Bureau de recherche
et développement

TECHNICAL MEMORANDUM 97/254
November 1997

**NONLINEAR FINITE ELEMENT ANALYSES OF
DAMAGED STIFFENED PANELS**

Thomas S. Z. Hu

19980126 141

DTIC QUALITY INSPECTED 2

**Defence
Research
Establishment
Atlantic**



**Centre de
Recherches pour la
Défense
Atlantique**

Canada

DISTRIBUTION STATEMENT A
Approved for public release;
Distribution Unlimited

DEFENCE RESEARCH ESTABLISHMENT ATLANTIC

9 GROVE STREET

P.O. BOX 1012
DARTMOUTH, N.S.
B2Y 3Z7

TELEPHONE
(902) 426-3100

CENTRE DE RECHERCHES POUR LA DÉFENSE ATLANTIQUE

9 GROVE STREET

C.P. BOX 1012
DARTMOUTH, N.É.
B2Y 3Z7



National Defence
Research and
Development Branch

Défense nationale
Bureau de recherche
et développement

**NONLINEAR FINITE ELEMENT ANALYSES OF
DAMAGED STIFFENED PANELS**

Thomas S. Z. Hu

November 1997

Approved by R. W. Graham:
Head/ Hydronautics Section

TECHNICAL MEMORANDUM 97/254

**Defence
Research
Establishment
Atlantic**



**Centre de
Recherches pour la
Défense
Atlantique**

Canada

Abstract

Ship hulls suffer various types of damage during operation. This damage can be corrosion caused by the marine environment or dents resulted from external forces. In order to make efficient repair decisions, residual strength of the damaged component needs to be assessed. The assessment can be carried out with numerical models such as nonlinear finite element methods or simplified approaches, but this requires experimental verification. DREA conducted a joint stiffened panel strength testing project with the U.S. Interagency Ship Structural Committee (SSC). Five stiffened panels in this project, having dimensions approximately equal to a typical stiffened panel at the upper deck of the Canadian Patrol Frigate (CPF), had deliberately created damage. Three of the panels had part of the web or flange of the stiffener removed while the other two had permanent deflection caused by large lateral forces. A series of finite element analyses were conducted to predict the collapse load as well as to simulate the buckling behavior. This memorandum summarizes the finite element results and their relation with the test observations. Some discussion and suggestions are also provided.

Résumé

Les coques de navire subissent divers types de dommages en service. Il y a la corrosion causée par le milieu marin ou des bosses causées par des forces externes. Pour pouvoir décider de façon efficace quelles réparations effectuer, il faut évaluer la contrainte résiduelle des composants endommagés. Cette évaluation peut être effectuée par des modèles numériques comme l'analyse par éléments finis non linéaires ou des approches simplifiées, mais une vérification expérimentale est nécessaire. Le CRDA a réalisé, conjointement avec l'Interagency Ship Structural Committee (SSC) des États-Unis, un projet d'essais de résistance de panneaux raidis. Dans le cadre ce projet, cinq panneaux raidis, de dimensions approximativement égales à un panneau raidi typique du pont supérieur de la frégate canadienne de patrouille avaient été délibérément endommagés. Sur trois d'entre eux, on avait enlevé une partie de l'âme du raidisseur, alors que sur les deux autres une flèche permanente avait produit des efforts latéraux importants. Une série d'analyses par éléments finis avait permis de prédire la charge d'effondrement et de simuler la tenue au flambage. Cette note résume les résultats de l'analyse par éléments finis et leur relation avec les observations des essais. Elle contient également une discussion et des suggestions.

DREA TM/97/254

Nonlinear Finite Element Analyses of Damaged Stiffened Panels

by

Thomas S.Z. Hu

Executive Summary

Introduction

Ship hulls suffer various types of damage during operation. The damage can be corrosion caused by the marine environment or dents resulting from external forces. In order to make an efficient repair decision, one needs to know the residual strength of the damaged components. The assessment can be carried out with numerical models, but this requires experimental verification. DREA conducted a joint stiffened panel strength testing project with the U.S. Interagency Ship Structural Committee. Five stiffened panels, having dimensions approximately equal to a panel at the upper deck of the Canadian Patrol Frigate (CPF), were tested, all having prior deliberately created damage. Three of the panels had part of the web or flange of the stiffener removed to represent corrosion while the other two had permanent deflection caused by large lateral forces. A series of finite element analyses were conducted to predict the residual strength as well as to simulate the behavior of the panels. This memorandum summarizes the finite element results.

Principal Results

Two specimens ("dented" panels) which had large permanent deflection at mid-span failed in a combined plate buckling and an overall flexural buckling mode. They were simulated very well with the finite element models. One of the "corroded" panels, in which the thickness of the flange at the mid-span was reduced but retained its structural continuity, was also simulated well with the finite element model. The other two "corroded" panels, having either part of the flange or part of the web cut-off, however, showed large discrepancies between finite element models and test results.

Significance of Results

Panels with various dents but retaining their structural continuity can be modeled with confidence. The corroded panels in which the corrosion penetrates the structural components are harder to predict. These discontinuities can cause rapid stress redistribution, induce higher stress gradient, and result in stress concentration in some areas. They might also induce large local plasticity or a large strain especially at the corners of the cut-out. Depending on the shape and location of the cut-out, a different mesh should be used. The results provide valuable information for future modeling of damaged components.

Future Plans

A refined mesh around the cut-out may be necessary to pick up the local behavior. However, great effort is required to redesign the mesh. DREA is currently developing an automatic mesh generator and enhancing the nonlinear finite element program VAST. The panels could be used as test cases and be rerun in the future. DREA is also developing a simplified approach based on a layered beam model to evaluate the ship hull strength. This model could be extended to include the local damage in the future.

Contents

Abstract	ii
Executive Summary	iii
Table of Contents	iv
List of Figures	v
List of Tables	v
Nomenclature	v
1. Introduction	1
2. Test Procedure	2
2.1 General	2
2.2 Test set-up and procedure	3
3. Finite Element Model	4
3.1 General	4
3.2 Boundary conditions and analytical procedure	4
4. Finite Element and Test Results	7
4.1 "Dented" panels	7
4.2 "Corroded" panels	8
5. Concluding Remarks	10
6. References	29

List of Figures

1. Coordinate system	11
2. Schematic plot of boundary devices	11
3. Test set-up	12
4. Side view of test set-up	13
5. End support	14
6. Corroded specimens	14
7. Boundary conditions of "corroded" panels	15
8. Boundary conditions of "dented" panels	16
9. Time functions of "dented" panels	17
10. Lateral load - lateral deflection curves of "dented" panels	18
11. Lateral load - end rotation curves of "dented" panels	19
12. Axial load - end shortening curves of "dented" panels	20
13. Deformations of SP2.2 at various load steps	21
14. Final deformed shapes of SP2.2	22
15. Load - shortening curves of SP3.2	23
16. Final deformed shapes of SP3.2	24
17. Load - shortening curves of SP3.1 and SP3.3	25
18. Final deformed shapes of SP3.1	26
19. Close up views of final deformed shapes of SP3.1	27
20. Final deformed shapes of SP3.3	28

List of Tables

1. Summaries of the finite element and test results of "dented" panels	7
2. Summaries of the finite element and test results of "corroded" panels	7

Nomenclature:

bf, bp	flange width, plate width
dw	web height
R_x, R_y, R_z	rotation about X, Y or Z axis
tf, tp, tw	flange thickness, plate thickness, web thickness
U_x, U_y, U_z	displacement in X, Y or Z axis

1. Introduction

Ship hulls suffer various types of damage during operation. This damage can be corrosion caused by the marine environment or dents resulting from external forces. In order to make an efficient repair decision, the residual strength of the damaged components needs to be assessed. The assessment can be carried out with numerical models such as nonlinear finite element analyses or simplified approaches, but all require experimental verification.

DREA conducted a joint stiffened panel strength testing project [1] with the U.S. Interagency Ship Structural Committee (SSC). Twelve single stiffened plates, having the dimensions approximately equal to a typical stiffened panel at the strength deck of the Canadian Patrol Frigate (CPF), were tested. The test specimens were divided into three groups:

- seven "as-built" specimens (SP1.x) under combined lateral and axial load;
- two "dented" specimens (SP2.x) that had permanent deflection induced by large lateral forces;
- three "corroded" specimens (SP3.x) that had part of the web or the flange removed to represent corrosion damage.

This project was carried out in the Center for Engineering Research (C-FER) laboratories in Edmonton Alberta.

As the scientific authority, the author and the scientists in C-FER planned the test procedure, designed the test set-up, conducted the test, and performed the nonlinear finite element analyses. The purpose of the analyses was to predict the collapse load and the behavior of the specimens. A technical memorandum [2] regarding the finite element simulation of seven undamaged specimens (SP1.x) has been completed. The results showed the nonlinear finite element method can produce load-shortening response and buckling shapes similar to those obtained experimentally.

At the same time, DREA is conducting a CRAD major project - "The Improved Ship Structural Maintenance Management" (ISSMM) project. The goal of this project is to provide a tool to assess the effects of various types of damage and degradation on the structural integrity of the CPF. One aspect of structural integrity that will be assessed is the ultimate strength of the ship hull girder. The author is responsible for developing tools to evaluate strength reduction caused by the damage. This memorandum presents the finite element results of the remaining specimens, two "dented" panels (SP2.x) and three "corroded" panels (SP3.x) in the C-FER test. The results will provide valuable information for development of future software and analytical techniques in the ISSMM project.

The details of the test set-up and procedure can be found in References 1 and 2. However, to assist in understanding the finite element modeling, the test set-up and procedure are briefly outlined in Section 2. The numerical models including the mesh division, boundary conditions, modeling techniques, and solution procedure are discussed in Section 3. The comparison of the finite element results with the test observations and discussion of the results are reported in Section 4.

2. Test Procedure

A detailed description of the test set-up and test procedure can be found in References 1 and 2. This section only summarizes those items that are important in the finite element modeling and analysis.

2.1 General

The test set-up was designed for single stiffened panels. Since the specimens represented a single stiffened panel cut out of a grillage between transverse frames, the test set-up was designed to be simply supported at both ends with symmetric boundary conditions along the sides. The mean values of the dimension of the specimen were $b_p \times t_p = 500.4 \text{ mm} \times 9.67 \text{ mm}$; $b_f \times t_f = 103.9 \text{ mm} \times 8.06 \text{ mm}$; and $d_w \times t_w = 136.8 \text{ mm} \times 6.22 \text{ mm}$. The length of the specimen was 2000 mm.

The stiffener was hot-rolled grade 350 WT tee section (nominal size 127 mm \times 102 mm) and the plate was made of hot-rolled 350WT steel. The stress-strain curves of the tension coupons cut from the plates, webs and flanges of the stiffeners showed a noticeable yield plateau of typical hot-rolled structural steel. The static yield stresses of different components of the stiffened panels were 425 MPa for the plate, 411 MPa for the web, and 395 MPa for the flange.

Longitudinal residual strains were measured using a sectioning method with mechanical gauges (100 mm gauge length). This method assumed that the longitudinal strains were uniformly distributed across the thickness and length. A total of 75 strips were cut from a 300 mm long segment. The measurements resulted in a residual stress pattern similar to that in a typical welded steel component. This pattern has a narrow tensile yield zone close to the weld, which sharply drops to compression at a short distance from the weld.

Before testing, the initial imperfections of the test specimens were measured for the "corroded" specimens (SP3.x) with a Nardini-SZ25120T lathe machine to provide a three-dimensional profile. Displacement gauges mounted on the carriage of the lathe machine traveled along the surfaces of the specimen to collect profile data at specified locations. There were in total 19 data points along the length of the panel and 5 lines across the panel including the junction of the web and the plate. The same numbers of data points were also measured along the length of the junction of the web and the flange, and along both edges of the flange. The imperfection data was referred to an orthogonal Cartesian coordinate system, as shown in **Figure 1**, with the panel located on the x-y plane. The origin of the plate was located at the mid-span of the junction of the plate and the web with the z-axis toward the toe of the Tee. The same coordinate system was used in the finite element model. Because the initial imperfections were very small in comparison to the permanent deformation caused by the large lateral forces, they were not measured for the "dented" specimens (SP2.x).

2.2 Test set-up and procedure

Since the panel represented a cut-out from a grillage between transverse frames, symmetric and simply-supported boundary conditions were assumed at sides and ends, respectively. Symmetric boundaries were simulated with five discrete devices along each side, as shown in **Figure 2**. The device was designed so that the edge of the plate is not allowed to rotate about the x- and z- axes. The test set-up is shown in **Figure 3**. Two hydraulic jacks attached to the wall applied the lateral load at the two third points through two 100 kN rams while the axial load was applied from the TTS (Tubular Testing System) head. The side view of the test set-up and the loading points are shown in **Figure 4**. Cylindrical bearings at both ends provided simple supports and transferred the reactions of the lateral load through friction. The details of the end supports are shown in **Figure 5**. It is important to note in the deformed configuration that the contact point between the cylinder and base plate (the lateral reaction point) moves transversely as the specimen deforms and the axial loading point always goes through point "o".

The permanent deflection at two damaged specimens SP2.1 and SP2.2 were created by large lateral forces under the TTS machine. An initial axial load of about 600 kN was applied on the specimen to generate enough friction force between the cylinder and the end plates to keep the specimen in place. The lateral loads were then applied on the specimen to create a dent. Permanent deflections at mid-span were 20 and 35 mm for SP2.1 and SP2.2, respectively. Both the lateral forces and the initial axial load were removed at the end of the "denting cycle". The axial load was then applied to determine the failure load and the buckling mode of the "dented" specimen.

The "corrosion" in the corroded specimens (SP3.x) is shown in **Figure 6**. The specimens SP3.1 and SP3.3 had a cut out in the web and flange, respectively, while SP3.2 had the thickness on part of its flange reduced. These specimens were placed under the TTS machine and compressed until collapse.

3. Finite Element Model

This section describes the finite element mesh, the modeling of the boundary conditions, and the modeling of the loads. The commercial finite element program ADINA [3] which enabled modeling of geometric and material non-linearities was used in this study.

3.1 General

A four-node quadrilateral shell element, from the family of the degenerate iso-parametric shell elements, with a $2 \times 2 \times 2$ integration order was used to model the plate and the stiffener. The kinematic assumption that was made was large displacement and rotation but small strain. Since the coupon tests had shown a clear plateau after yielding, the material modeling of the plate was assumed to be bilinear elastic-perfectly-plastic with a von Mises yield condition.

For the “corroded” panels, the imperfections of the finite element model were directly mapped [2] from the test measurements with linear interpolation and extrapolation. Since the initial imperfections were small in comparison with the permanent deformations caused by the large lateral forces in the “dented” panels, they were not measured in the test. However, the profile of an “as-built” specimen, SP1.2 tested earlier, was used as the initial imperfection.

In considering the boundary supports and the residual stress pattern, a finer mesh was used so that the nodal points would coincide with the boundary gripping devices. The final mesh sizes were 16×38 for the plate; 6×38 for the web; and 4×38 for the flange.

The co-ordinate system for the finite element model was the same as for the test measurement. It refers to an orthogonal Cartesian co-ordinate system with the mid-plane of the plate located in the x-y plane. The origin was located at the mid-span of the model at the junction of the web with the plate parallel to the x-axis. The positive z-axis was toward the junction of the toe of the stiffener. The mesh was designed so that each grip fixture contained two elements. The grip fixture was modeled with two thicker elements on top of the plate and was restrained against rotation in the x- and z- directions.

The residual stresses were generated through temperature variations on nodal points adjacent to the weld. The magnitude of the residual stress was calibrated by changing the temperature magnitude. A procedure used in Reference [4] for the automatic generation of welding residual stresses with retention of the initial imperfections was used.

3.2 Boundary conditions and analytical procedure

As shown in **Figure 1**, specimens were welded between two thick end plates. These end plates ensured the ends remained plane during deformation. These plates were not modeled physically but “the plane sections remain plane” condition was achieved by assigning the end nodes to be slave nodes so they could displace together with respect to a master node.

As indicated in **Figure 4**, the specimen was mounted between two cylindrical heads. There was a distance (38.1 mm) between the center of the half-cylinder and the end of the specimen. When the plate started to buckle under the axial load, a slight eccentricity developed. To account for this eccentricity, the master node was offset 38.1 mm from the end of the plate.

The boundary conditions for the “corroded” panel are shown in **Figure 7**. The “corroded” part in the model was produced either by removing the elements or reducing the element thickness in the “corroded” portions without altering the mesh. In other words, a coarse mesh was used around the cut-out.

The modeling of “dented” panels was more complicated. Since the lateral reaction points as shown in **Figure 4** were located at the contact points of the cylinders and the base plate, a pair of equivalent secondary end moments, caused by the initial axial load and by the offset of the lateral force reaction point, were developed at the master nodes. The magnitude of these moments changed along with the deformation of the panel. It was, therefore, necessary to include the cylinders into the finite element model. As shown in **Figure 8**, two large beams were used to connect the master nodes to the lateral load reaction points. The two reaction points were not allowed to move in the y- and z- directions when the model was subjected to lateral forces. To avoid unwanted lateral reaction forces, they were released when the model was subjected to axial load.

Non-linear collapse analysis was done by applying either “force” or “displacement” loading in small load steps. An iteration procedure was then used to achieve convergence. The finite element modeling of the test procedure involved several time functions such as temperature, lateral and axial loading. A total of fifty time steps were used in the simulation. Because of changing the boundary conditions as well as the applied loading control methods, several restart runs were needed for the “dented” panels.

For the “corroded” model, the axial displacement loading was applied after generating the desired residual stresses and imperfections. The procedure was more complicated for the “dented” model. The time function for this model is shown in **Figure 9**. Temperature loading was applied throughout the analysis. An initial axial force loading equivalent to 600 kN was applied linearly from step 0 to step 4. It was maintained as a constant until step 20. Because of the secondary moment caused by the initial axial load, the lateral load-lateral displacement curve was expected to have a descending branch after the peak lateral force. Therefore, the displacement loading control method was used in the “denting” cycle. The lateral displacement loading was applied at step 5 and increased linearly until step 13.

One problem arose at this step. If the solution method changed to “force” loading control, the solution would converge back to the previous load path. On the other hand, if the decreased “displacement” control method was used, one would need to know the lateral permanent deflection in which the lateral reaction forces would be equal to zero. Therefore, it was decided to use the decreased “displacement” loading control method to force the curve to follow the unloading branch, replace the “displacement” loading with an equivalent

“force” loading, and shift to the decreased “force” loading control method. By following these steps, the decreased displacement control method was used until load step 15 in which the lateral load was half way into the unloading branch. A pair of equivalent lateral forces, that would create the same deflection in step 15, was applied to the model in a restart run and linearly decreased until step 20 in which the lateral load was equal to zero. The initial axial load was then decreased linearly to step 23. The permanent lateral deflection at mid-span was compared to the test result. The procedure was repeated until the desired permanent deflection was obtained. After obtaining the satisfactory deflection, the axial load was applied until the collapse of the panel.

The restart runs were divided according to the changing boundary conditions and loading control methods. The first run was from step 0 to step 15. The second run was from step 15 to step 23 in which the lateral forces changed from displacement loading to force loading. The boundary conditions were changed, as shown in **Figure 8**, at the third run to prevent unwanted reaction forces caused by the axial load.

4. Finite Element Results

Five panels have been analyzed and compared with the test results. The finite element and the test results of “dented” specimens (SP2.x) and “corroded” specimens (SP3.x) are summarized in Tables 1 and 2, respectively.

Table 1: Summaries of the finite element and test results of “dented” panels

Specimen No.	peak lateral load (kN)	peak lateral deflection (mm)	permanent lateral deflection (mm)	peak axial load (kN)	failure mode
SP1.2 Test	-	-	-	1736	flexural
SP1.2 FEA	-	-	-	1759	flexural
SP2.1 Test	71.46	33.21	19.97	1331	flexural
SP2.1 FEA	74.26	37.42	19.18	1348	flexural
SP2.2 Test	72.40	53.03	35.51	1116	flexural
SP2.2 FEA(1)	74.45	53.55	39.87	1120	flexural
SP2.2 FEA(2)	74.30	48.84	35.15	1200	flexural

- the second run of SP2.2 (2) has a permanent deflection approximately equal to the test while the first run SP2.2(1) has a peak deflection similar to the test.
- SP1.2 is an “as-built” specimen and has no permanent deflection.

Table 2: Summaries of the finite element and test results of “corroded” panels

	Test		FEA	
	peak load (kN)	failure mode	peak load (kN)	failure mode
SP1.2	1736	flexural	1759	flexural
SP3.1	1635	plastic hinges	1727	flexural
SP3.2	1773	flexural	1760	flexural
SP3.3	1683	tripping	1765	flexural

- SP1.2 is an “as built” specimen.
- SP3.1 has a cut-out on the web while SP3.3 has a cut-out on one side of the flange.
- SP3.2 has the flange thickness reduced on both side.

One of the specimens, SP1.2, shown in the tables is an “as-built” specimen analyzed previously [2]. This specimen has no lateral load and no damage. The results of this specimen will be used as the baseline for the comparison. This section describes the comparison between the test observations and analytical behavior.

4.1 “Dented” panels

Before the axial loading cycle, specimens SP2.1 and SP2.2 underwent a “denting” cycle. A 600 kN initial axial load was applied to achieve enough friction between the loading heads

and the end plates of the specimens, followed by large lateral loads in the +z direction to create lateral deflection. The lateral forces and the initial axial load were then removed. The removing of the applied loading caused the panel to partially spring back. Permanent deflections of 19.97 and 35.51 mm for SP2.1 and SP2.2, respectively, remained at mid-span.

Because of the nonlinear nature of the analysis, a trial and error process was needed to produce the desired permanent deflection. Each specimen was analyzed several times. Table 1 shows two results for specimen SP2.2. The first one had the same peak lateral deflection as that in the test while the second run had a similar permanent deflection at mid-span. The lateral load- lateral deflection curves for SP2.1 and SP2.2 are shown in **Figure 10**, while the lateral load-end rotation curves are shown in **Figure 11**. It is important to note that the slope of the elastic region of the lateral load-lateral deflection curves of the test in the “denting” cycle does not match that calculated from the elastic theory. In contrast, the finite element results showed good agreement with the elastic prediction. The slope of the end rotations of both test and finite element method agree very well with the calculation based on the elastic theory.

The discrepancy in the deflections might be caused by faulty electronic recording devices or by the way that the testing data were extracted. The differences between the lateral peak load of the finite element analyses and test results are less than 4%. **Figure 12** shows the comparisons of the load-shortening curves. The differences in the peak loads are 2% for SP2.1 and 8% for the second run of SP2.2, respectively.

Both specimens and finite element models failed in a combined plate buckling and an overall flexural buckling mode. **Figure 13** shows the deformations at various load steps for SP2.2(2). The comparison of the final deformed shape of the SP2.2 test results with SP2.2(2) is shown in **Figure 14**. Compared to specimen SP1.2, the peak loads decreased by 23% and 36% for SP2.1 and SP2.2 in the test, respectively, while the decreases were 23% and 32% in the finite element analysis.

4.2 “Corroded” panels

Except for SP3.2, the finite element analyses for the “corroded” panels showed large discrepancies between the finite element results and the test observations. Although specimen SP3.2 had part of the thickness of its flange reduced, its structure still maintained continuity. The comparison of the load-shortening curves is shown in **Figure 15** for this specimen. The difference of the peak load is less than 1%. **Figure 16** shows the final failure mode of the test and the finite element analysis in which both failed in a combined plate buckling and overall flexural buckling mode. Compared to specimen SP1.2, reducing the flange thickness symmetrically in this case made no difference in terms of failure mode and load capacity.

Specimen SP3.1 had a 205 mm × 75 mm rectangular cut-out at the center of the web. During the test, this opening caused a sudden collapse when the upper portion of the specimen

snapped away from the lower portion in such a way that plastic hinges formed at the four corners of the cut-out. As shown in **Figure 17(a)**, the axial load - shortening curve had a sudden drop as the panel collapsed. The axial load decreased and snapped back immediately after reaching the peak load to about 500kN. However, the load - shortening curve of the finite element analysis did not resemble the test observation. The comparison of the overall failure modes is shown in **Figure 18**. A close look at the cut-out location is shown in **Figure 19**. No plastic hinge formed at corners of the cut-out in the finite element analysis. The panel failed in a combined plate buckling and overall flexural buckling mode.

Specimen SP3.3 had a 205 mm \times 25 mm cut-out from one side of the flange. During the test, the stiffener bent, twisted and failed in a tripping mode. Although it only decreased the peak load slightly, the load decreased sharply beyond the peak load as shown in **Figure 17(b)**. The finite element results showed a different behavior. The drop was less dramatic as the panel failed in a combined plate buckling and an overall flexural buckling mode. The comparison of the final deformed shapes is shown in **Figure 20**.

The final deformed shapes of SP3.1 and SP3.3 in the finite element analysis are combined plate buckling and overall flexural buckling modes. Unlike their counterparts in the test, the failure mode is identical to that of SP1.2 - an "as-built" specimen. It strongly suggested that the mesh around the cut-out was not appropriate to catch the local behavior.

5. Concluding Remarks

Five stiffened plate specimens, including two "dented" panels and three "corroded" panels, have been analyzed with the commercial finite element program ADINA. The analytical results agreed very well with the test observation in some cases but differed in others.

Since the test involved heavy machinery including loading and boundary devices, one should expect some uncertainties associated with these devices. These uncertainties could cause some variation in the test results. The finite element method, which models a continuous solid with discrete elements, is an approximation. Discrepancies between test observations and finite element results are expected. The differences, however, are unacceptable for specimens SP3.1 and SP3.3.

There are numerous books and papers regarding nonlinear finite element modeling techniques, accuracy and limitations in various aspects such as element types, meshing design, shape functions and solution methods. Generally speaking, a finite element model based on the displacement formulation is always stiffer than the real structure. The shape function used in the element formulation, limitations inherited from the small strain theory, and deficiencies existed in the load-displacement approach will prohibit an exact duplication of the test results. On the other hand, a particular problem can be modeled in different ways by users with different backgrounds. Understanding the structural behavior and knowing the finite element theory are essential to a successful analysis.

As far as these particular specimens are concerned, the finite element method can simulate the test results well if the panels maintain their structural continuity. On the other hand, a carefully planned mesh around the cut-out is necessary to represent the rapidly changing stress field and the local deformation. Since large strain and local plasticity were formed in the corners of the cut-out in specimens SP3.1 and SP3.3, a more refined mesh around the cut-out should provide better results.

The local mesh refinement requires a lot of time on the part of the finite element analyst. DREA is currently developing an automatic mesh generator with the goal of being able to refine local mesh with a mouse click. Hopefully, models of SP3.1 and SP3.3 with different mesh arrangements can be analyzed so that criteria for meshes around a cut-out in the nonlinear analysis can be established in the future.

DREA is also developing a simplified analytical model based on a layered beam formulation[5]. It is similar to the UK's program FABSTRAN [6] and is intended to replace DREA's program ULTMAT[7]. The CFER test results will be used to verify this simplified model. The overall goals of this development are to be able to analyze single stiffened panels and to calculate the ultimate collapse moment of a hull. Other components such as the intersections of deck and side, and deck and bulkhead, and grillages, in which several panels collapse as a whole, should also be tested and analyzed. A parametric study regarding the size and location of damage on "dented" panels should also be conducted in the future.

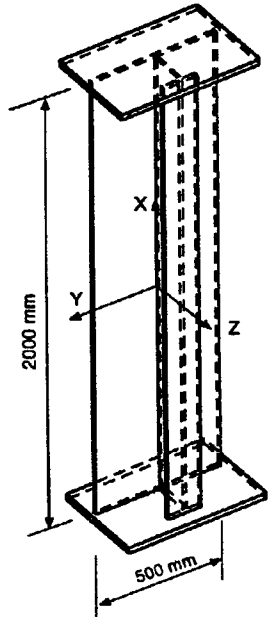


Figure 1: Coordinate system

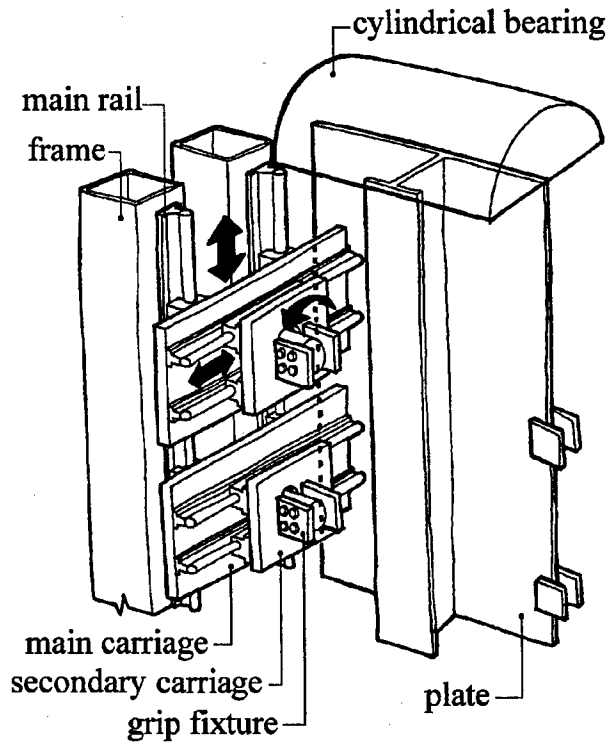


Figure 2: Schematic plot of boundary devices

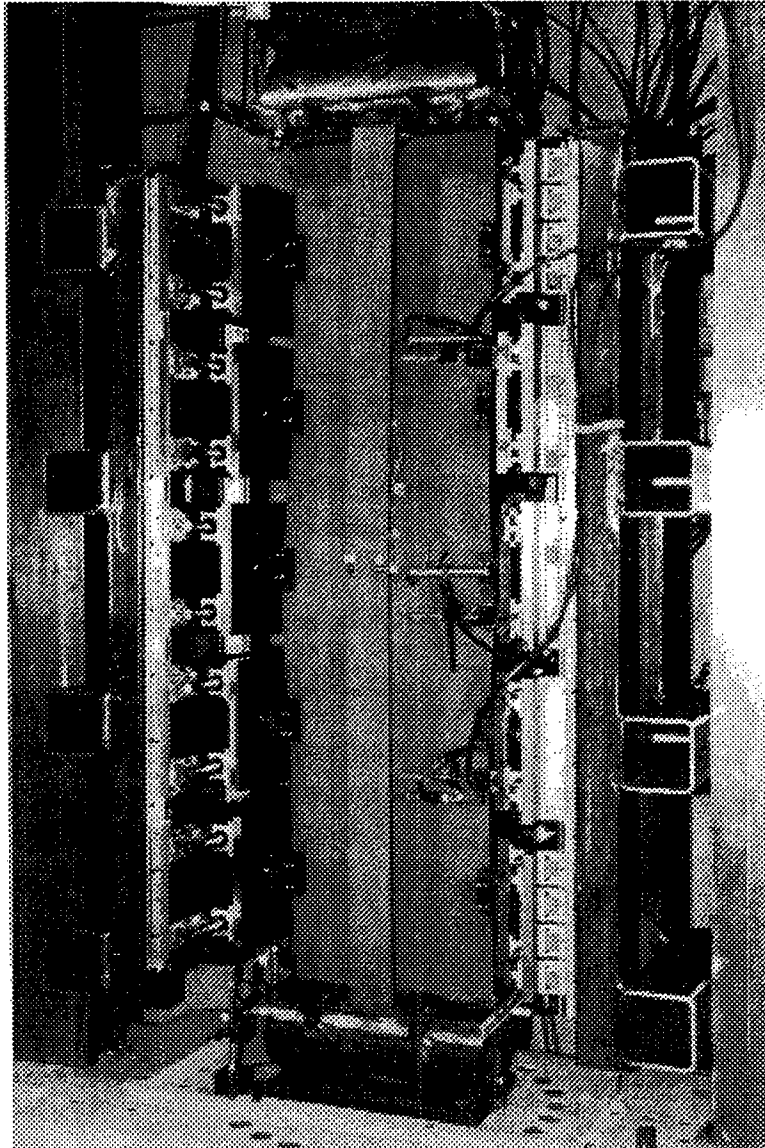


Figure 3: Test set-up

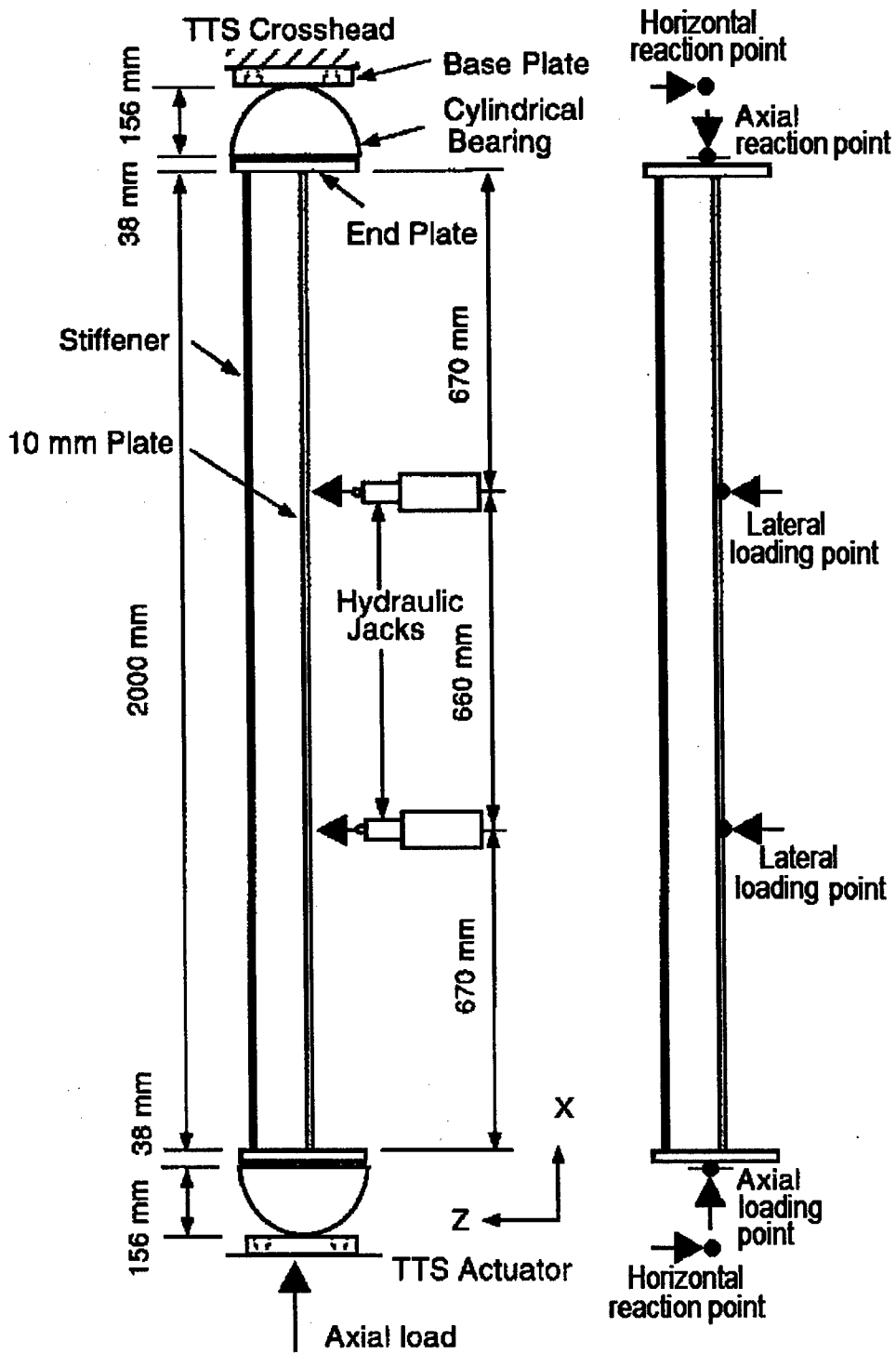


Figure 4: Side view of test set-up

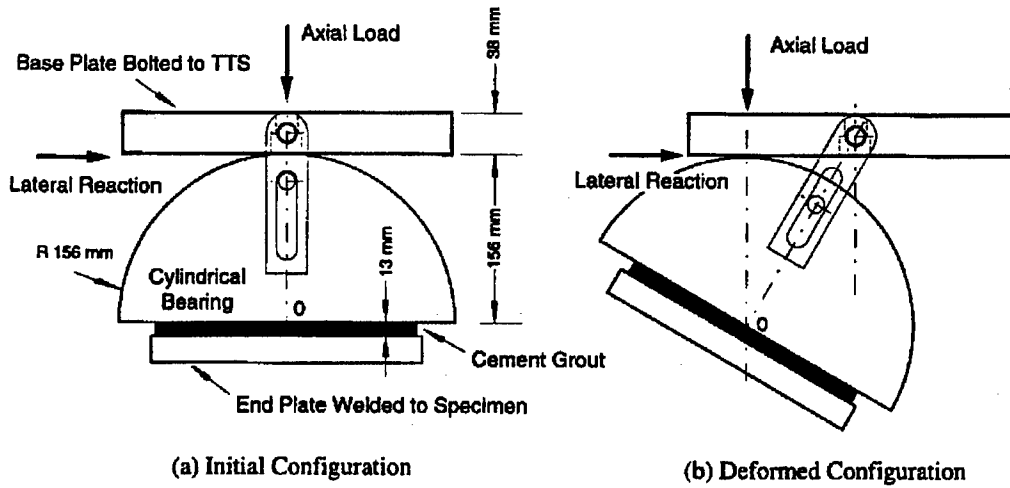


Figure 5: End support

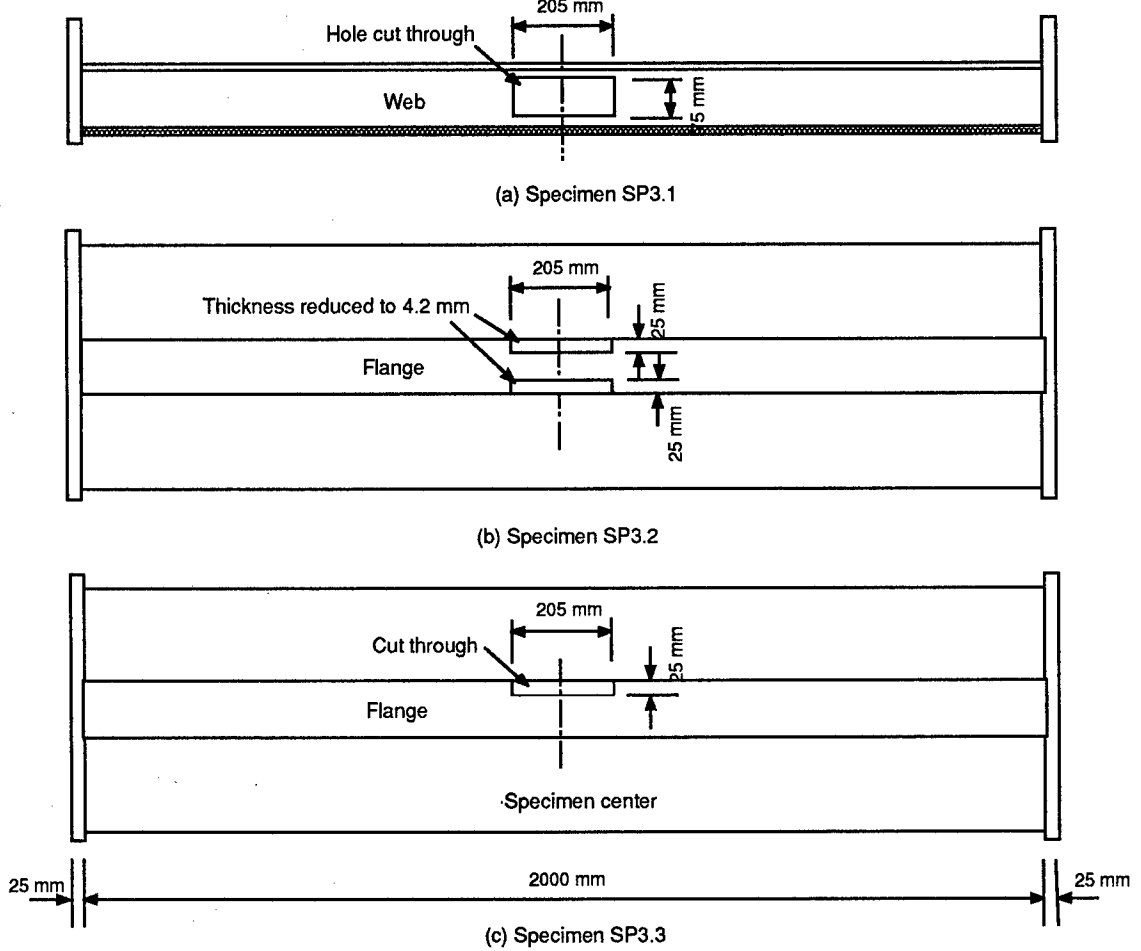


Figure 6: Corroded specimens

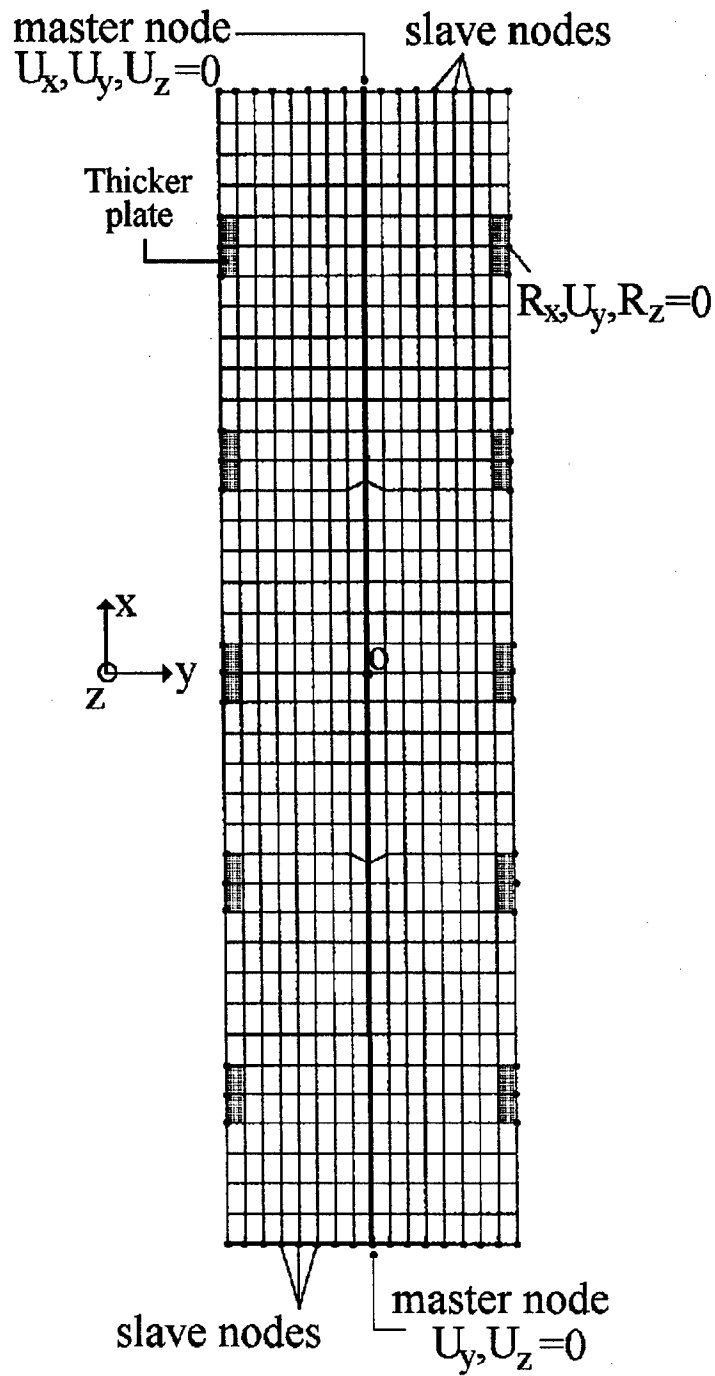


Figure 7: Boundary conditions of "corroded" panels

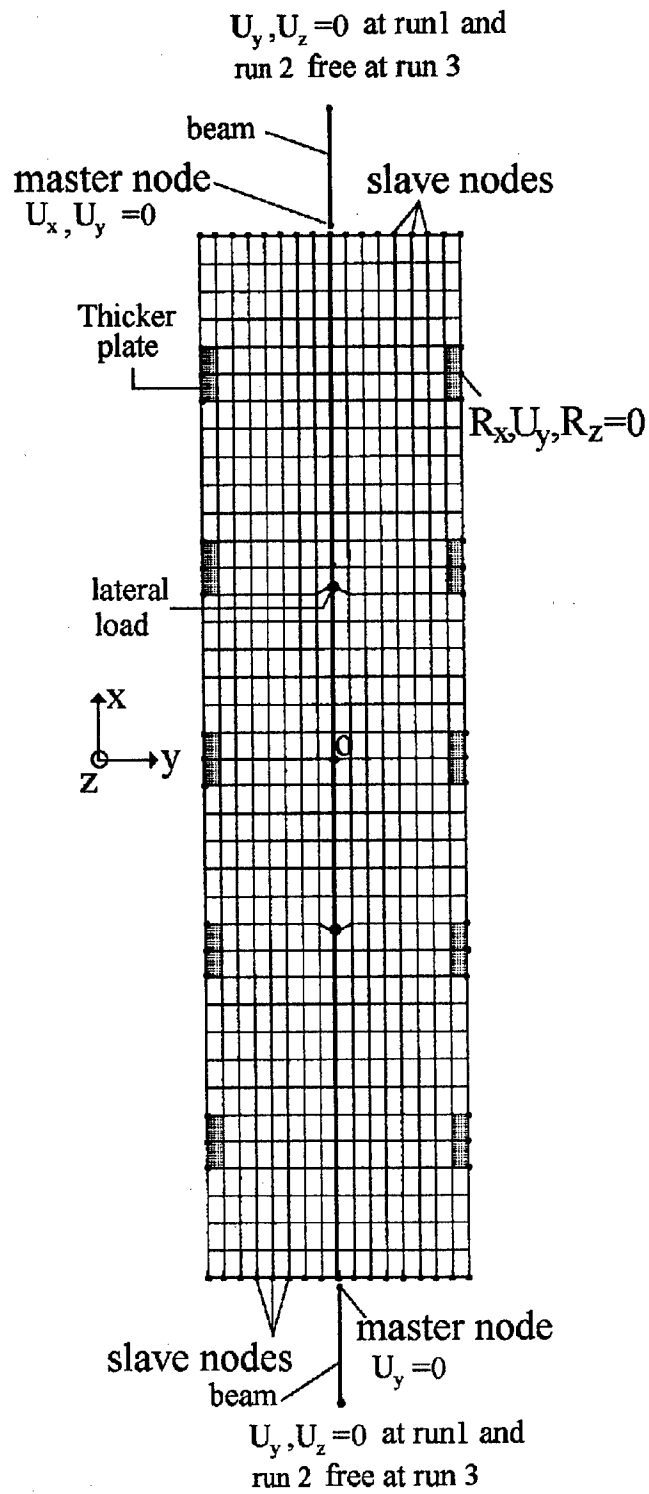


Figure 8: Boundary conditions of "dented" panels

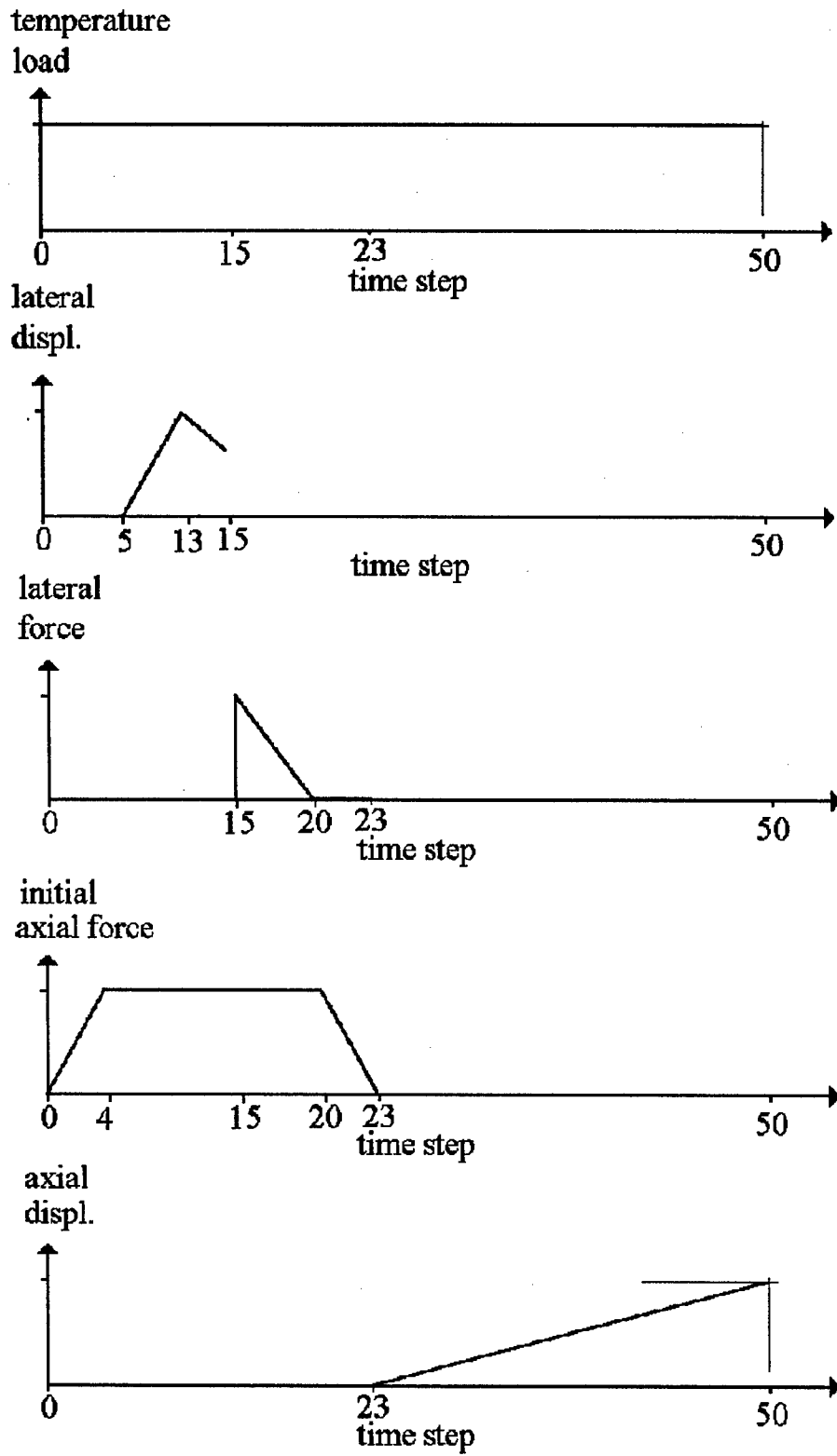
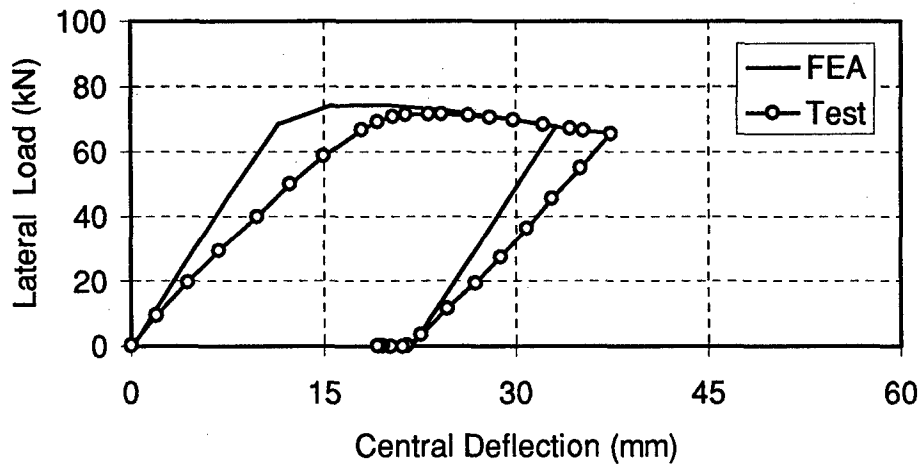
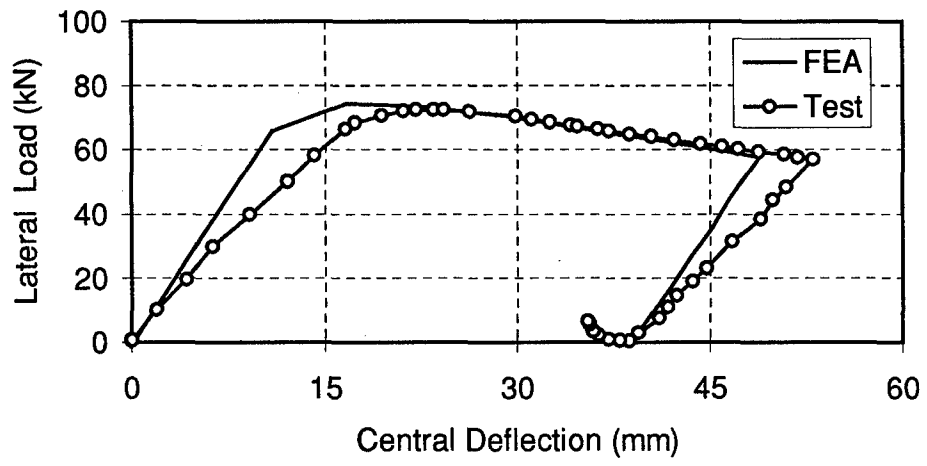


Figure 9: Time function of "dented" panels

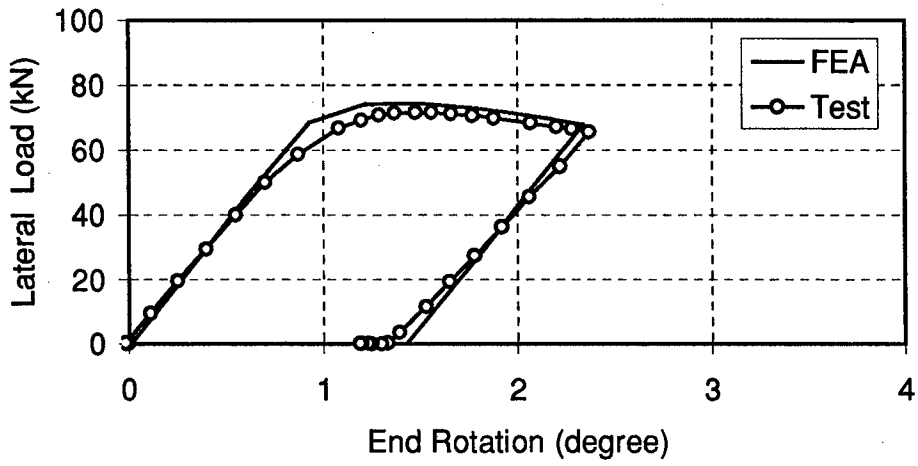


(a) SP2.1

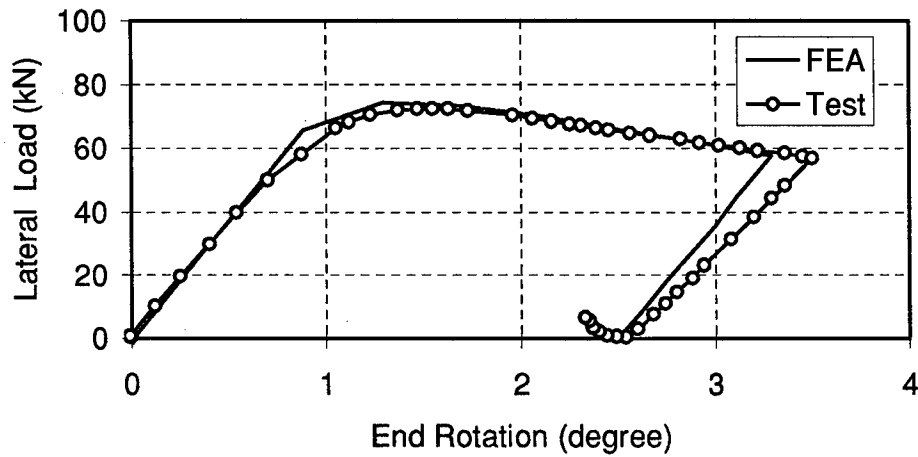


(b) P2.2(2)

Figure 10: Lateral load - lateral deflection curves of “dented” panels

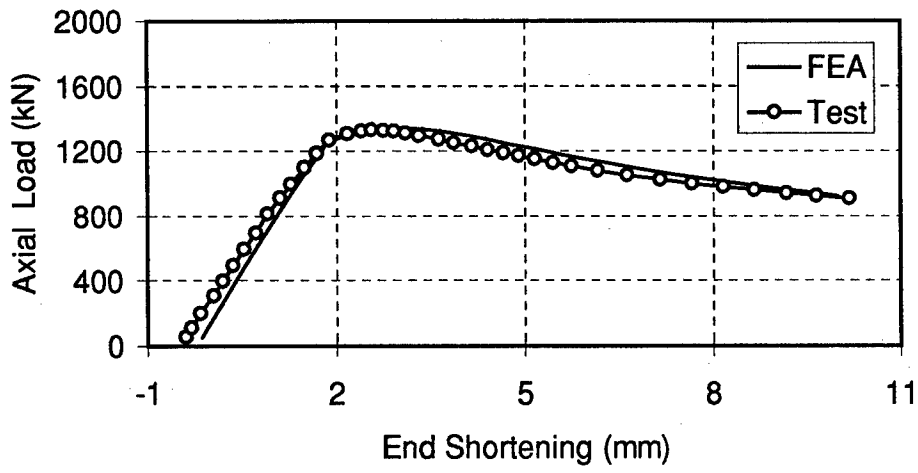


(a) SP2.1

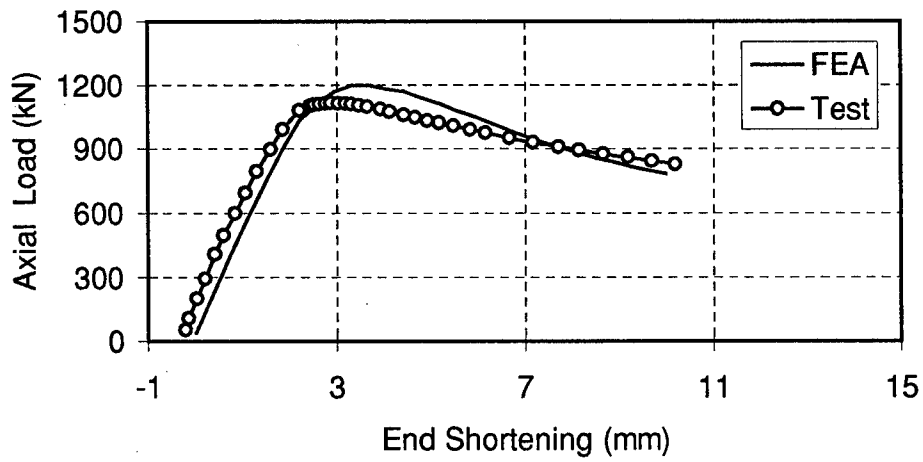


(b) SP2.2(2)

Figure 11: Lateral load - end rotation curves of "dented" panels



(a) SP2.1



(b) SP2.2(2)

Figure 12: Axial load - end shortening curves of “dented” panels

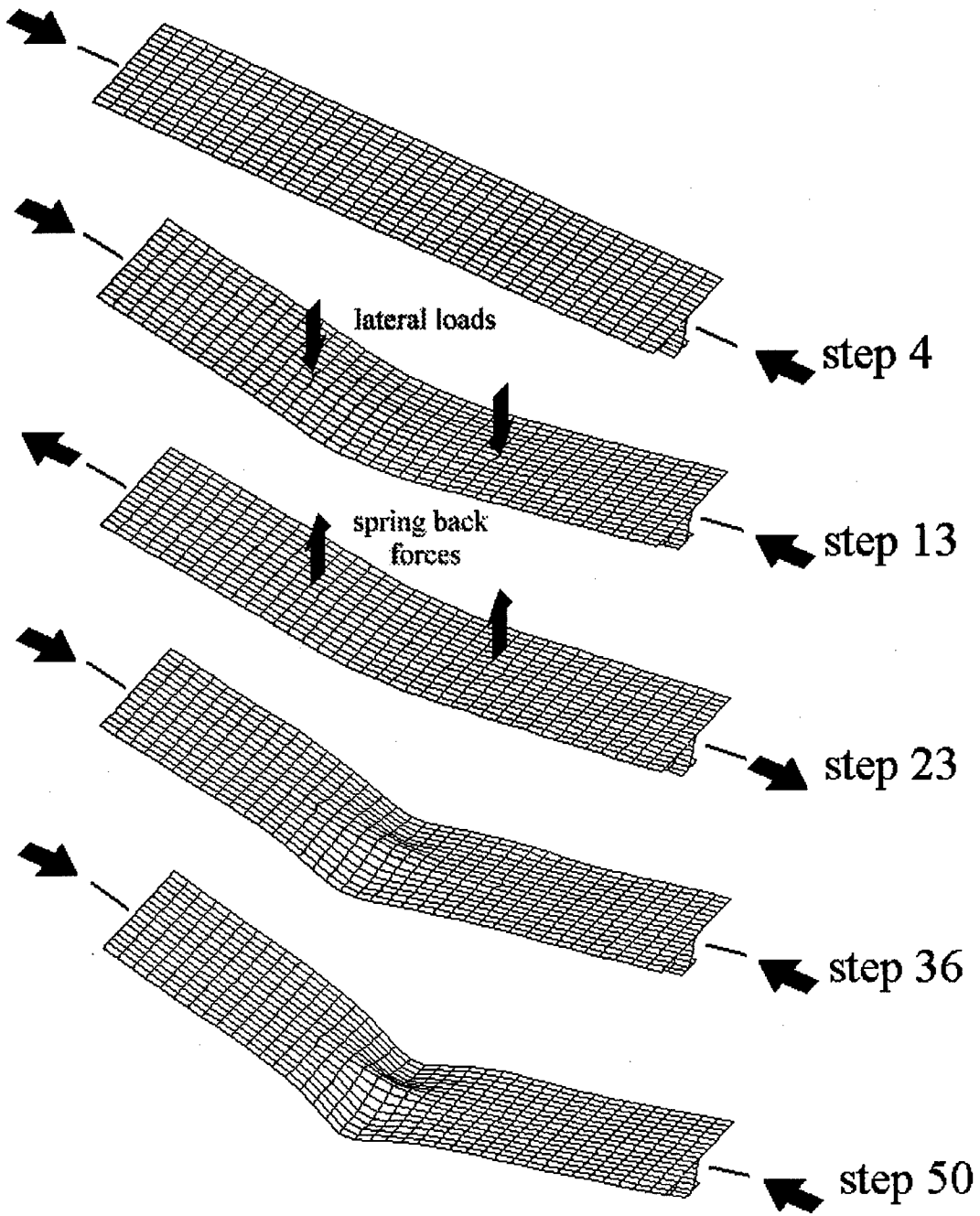


Figure 13: Deformations of SP2.2 at various load steps

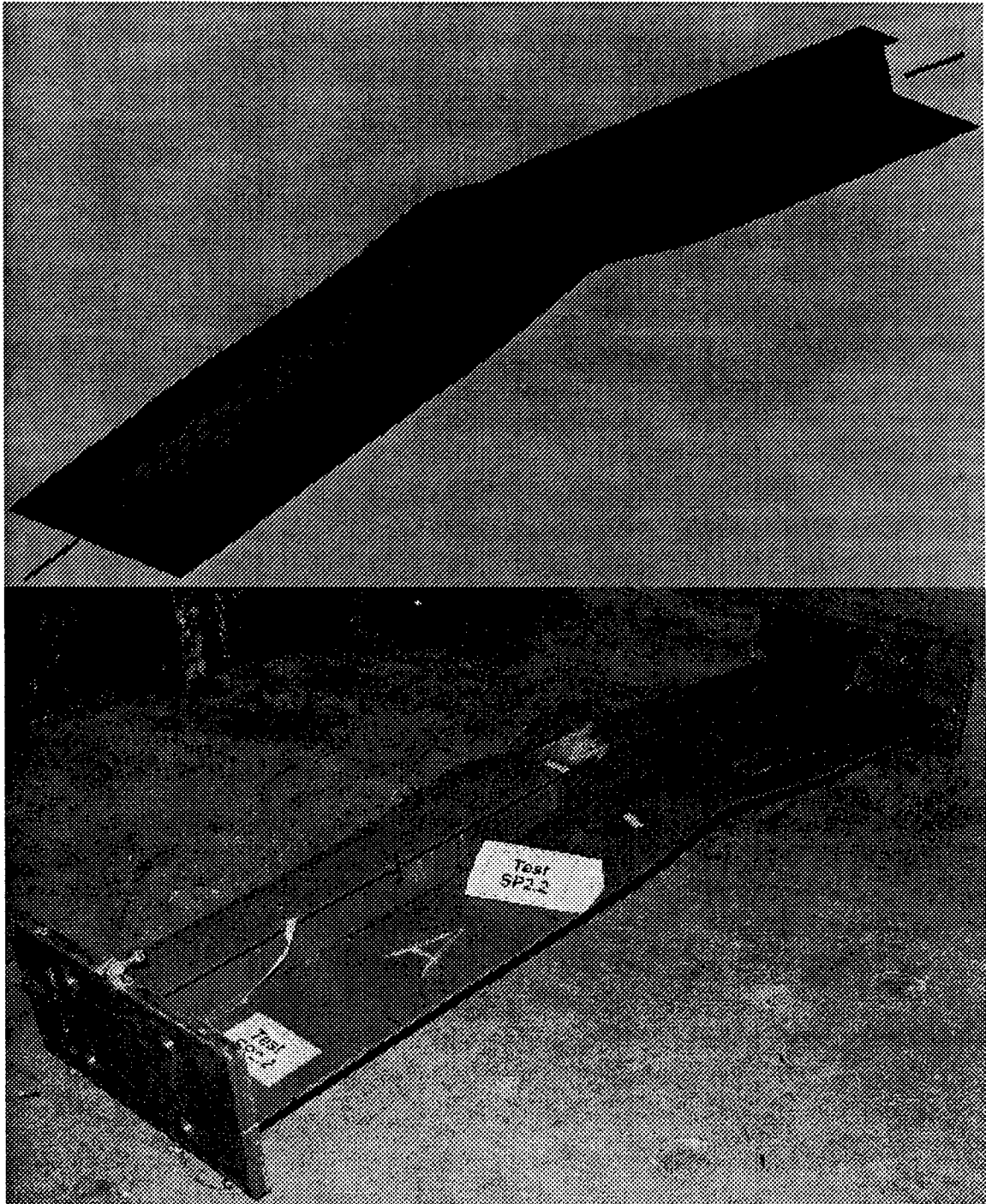


Figure 14: Final deformed shapes of SP2.2

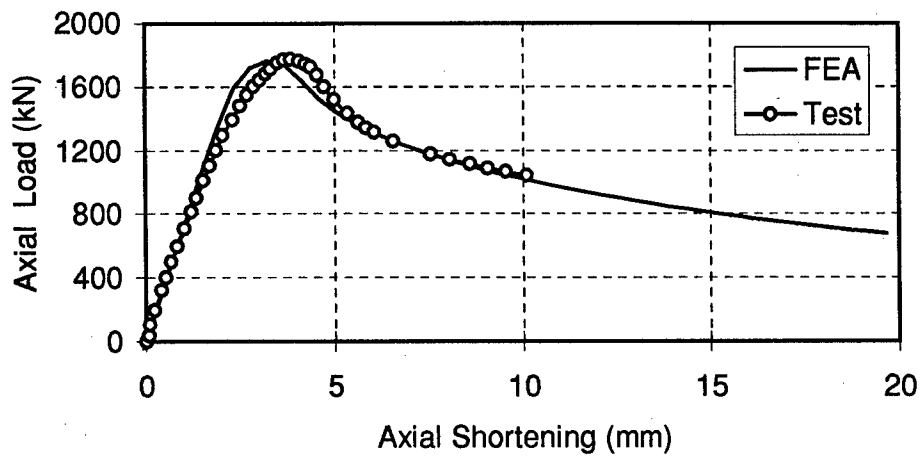


Figure 15: Load-shortening curves of SP3.2

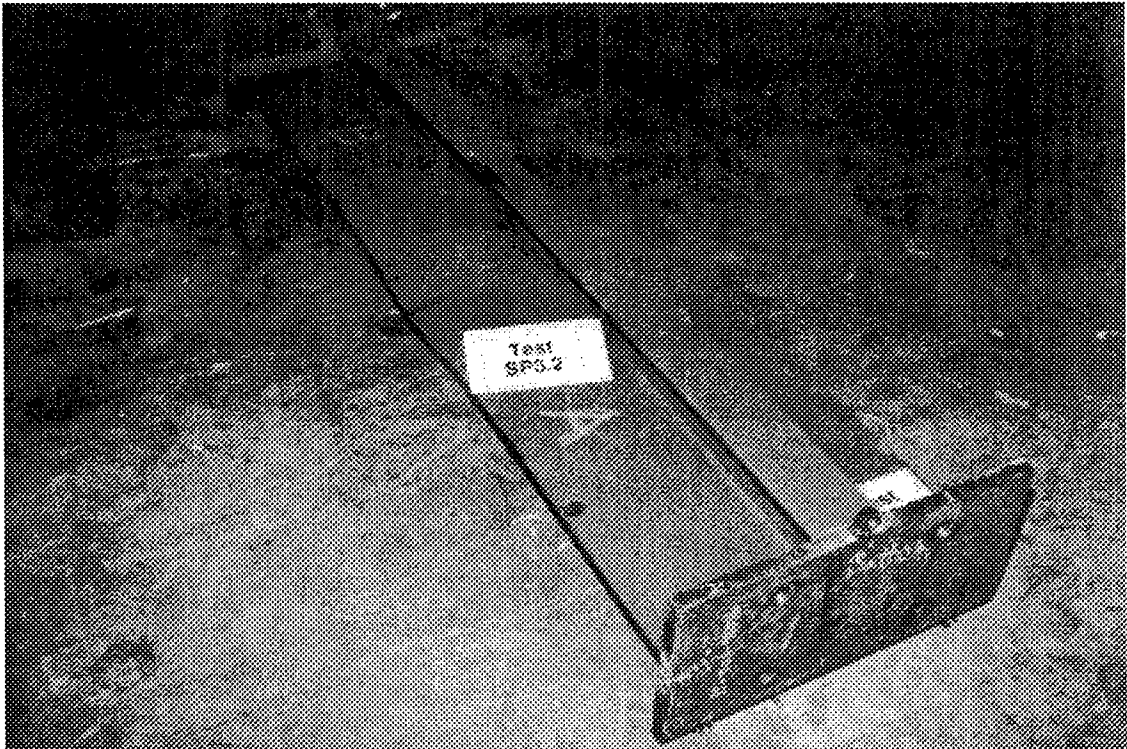
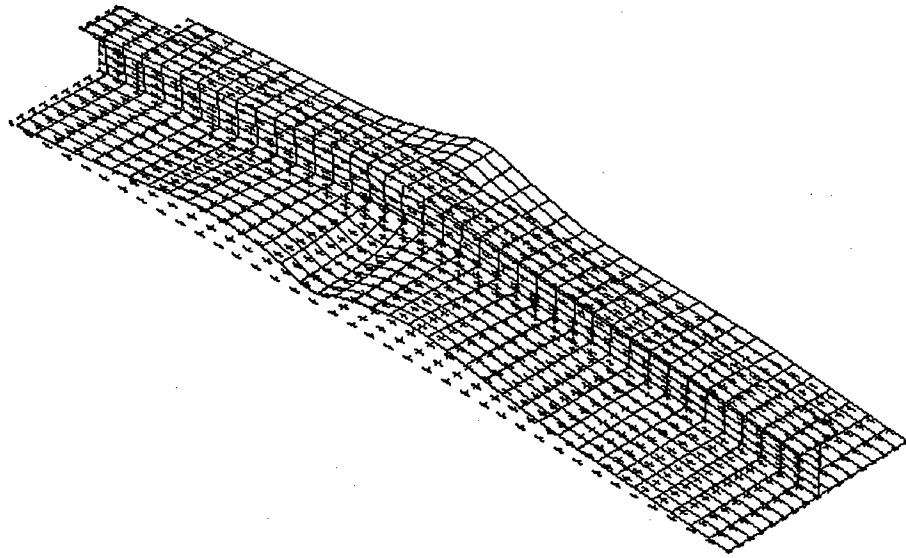
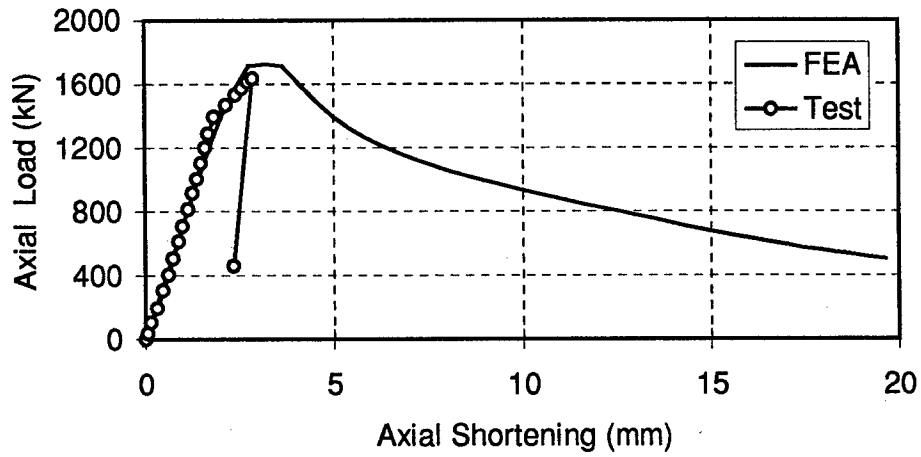
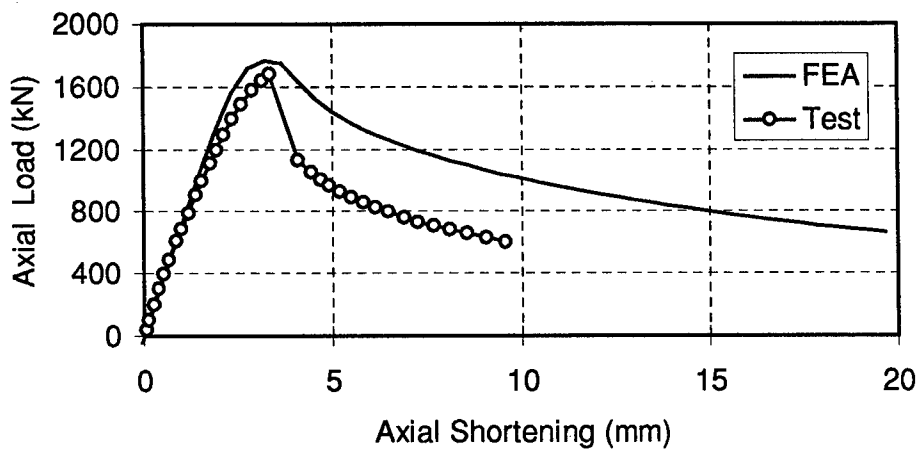


Figure 16: Final deformed shapes of SP3.2



(a) SP3.1



(b) SP3.2

Figure 17: Load-shortening curves of SP3.1 and SP3.3

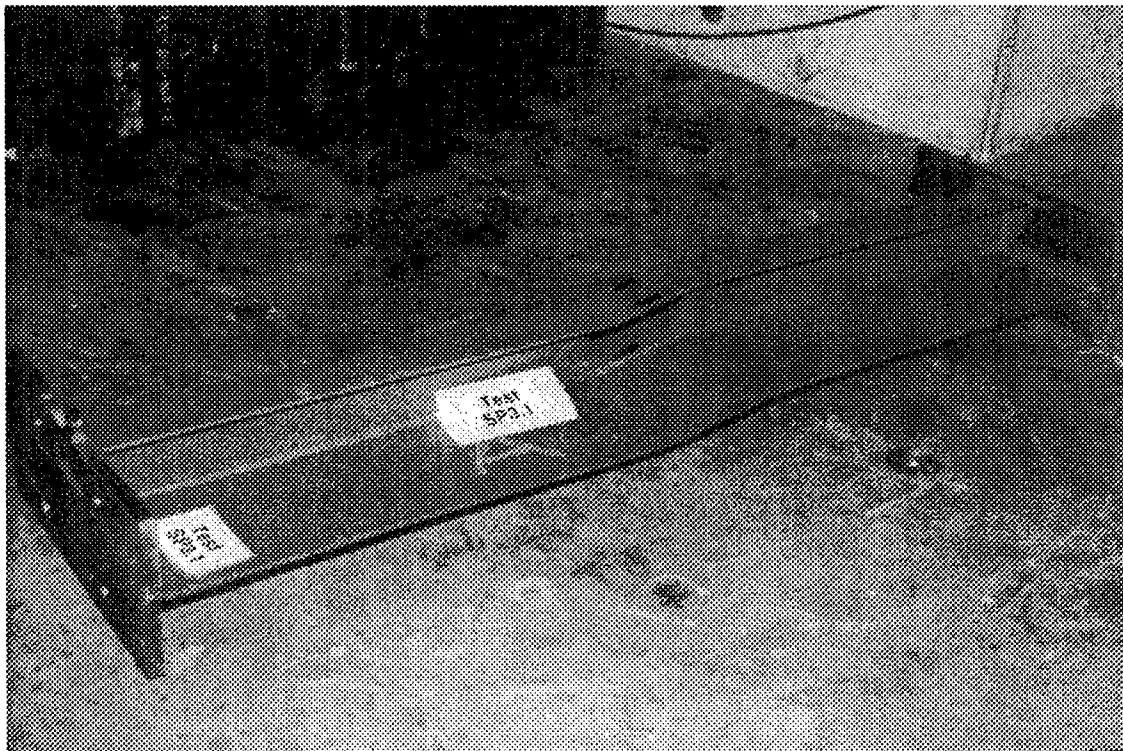
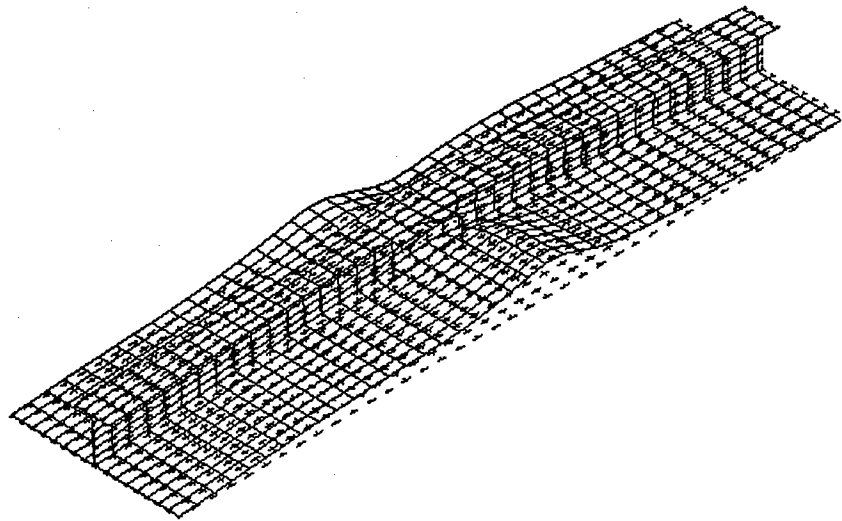


Figure 18: Final deformed shapes of SP3.1

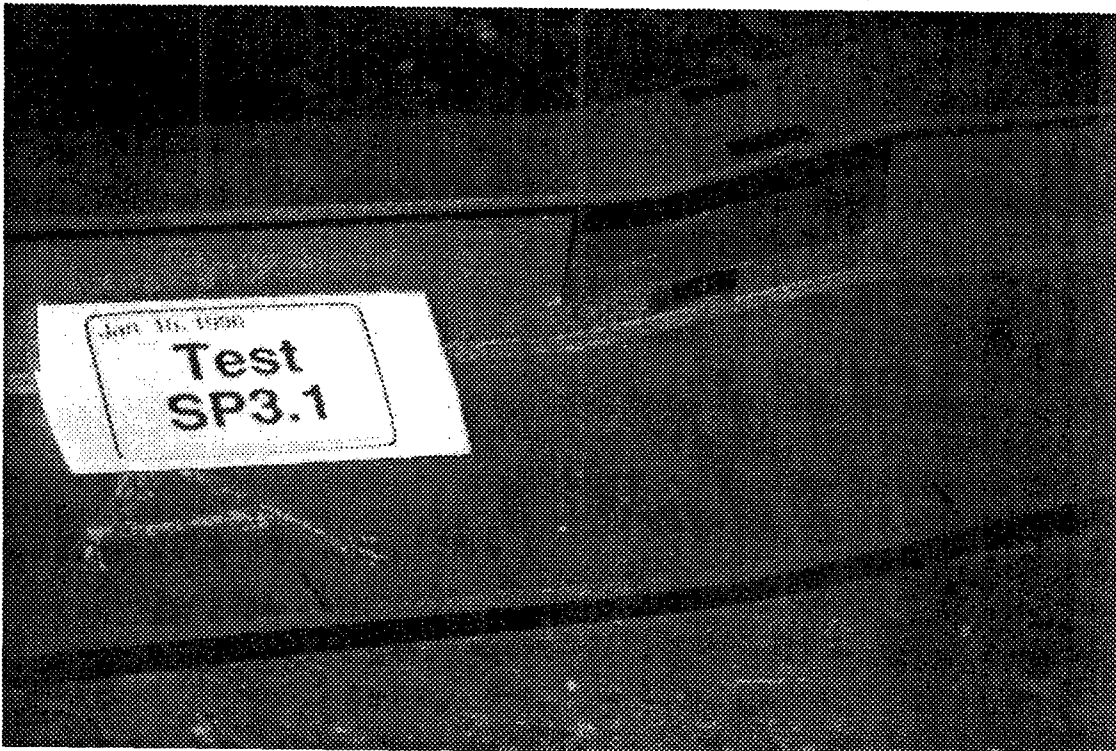
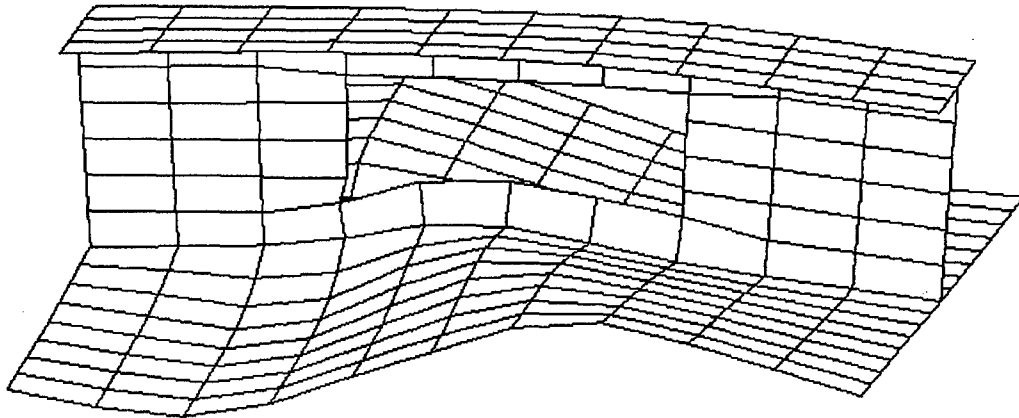


Figure 19: Close views of final deformed shapes of SP3.1

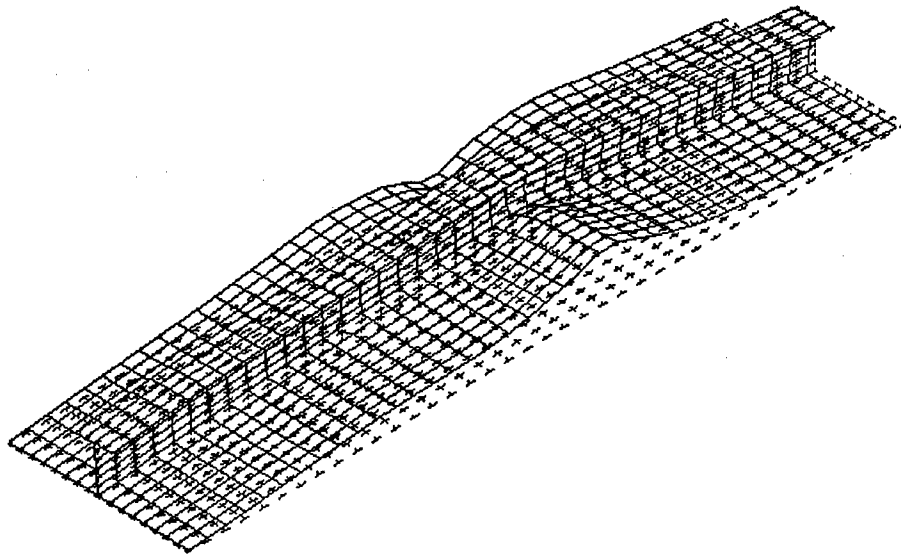


Figure 20: Final deformed shapes of SP3.3:

6. References

1. Chen, Q., Zimmerman, T.J.E., DeGeer, D. and Kennedy, B.W., "Strength and Stability Testing of Stiffened Plate Components", Ship Structural Committee Report SSC-399, 1997.
2. Hu, S.Z., "Nonlinear Finite Element Simulation of the Test Procedure for Stiffened Panels under Combined Lateral and In-plane Loads", DREA Technical Memorandum 97/219, March 1997.
3. "ADINA-IN for ADINA Users Manual", Report ARD 90-4, ADINA R & D, Inc., Sept. 1990.
4. Hu, S.Z., "An Analytical Investigation of the Compressive Behaviour of Fabricated Steel Tubes", Ph.D. Dissertation, Dept. of Civil Engineering, University of Toronto, 1991.
5. Owen, D.R.J. and Hinton, E., "Finite Elements in Plasticity: Theory and Practice", Pineridge Press Limited, UK, 1980.
6. Dow, R.S. and Smith, C.S., "FABSTRAN: A Computer Program for Frame and Beam Static and Transient Response Analysis (Nonlinear)", unpublished ARE (Admiralty Research Establishment) report, Dec. 1986.
7. Hu, S.Z., "EBMS - A Program for Equivalent Beam Modelling of Ship Structure", DREA Technical Memorandum 95/208, April 1995.

UNCLASSIFIED
 SECURITY CLASSIFICATION OF FORM
 (highest classification of Title, Abstract, Keywords)

DOCUMENT CONTROL DATA		
(Security classification of title, body of abstract and indexing annotation must be entered when the overall document is classified)		
1. ORIGINATOR (the name and address of the organization preparing the document.. Organizations for whom the document was prepared, e.g. Establishment sponsoring a contractor's report, or tasking agency, are entered in section 8.) Defence Research Establishment Atlantic PO Box 1012, Dartmouth, NS, Canada B2Y 3Z7	2. SECURITY CLASSIFICATION (overall security classification of the document including special warning terms if applicable). Unclassified	
3. TITLE (the complete document title as indicated on the title page. Its classification should be indicated by the appropriate abbreviation (S,C,R or U) in parentheses after the title). Nonlinear Finite Element Analyses of Damaged Stiffened Panels		
4. AUTHORS (Last name, first name, middle initial. If military, show rank, e.g. Doe, Maj. John E.) Hu, Thomas S. Z.		
5. DATE OF PUBLICATION (month and year of publication of document) November 1997	6a. NO. OF PAGES (total containing information include Annexes, Appendices, etc.) 36	6b. NO. OF REFS (total cited in document) 7
7. DESCRIPTIVE NOTES (the category of the document, e.g. technical report, technical note or memorandum. If appropriate, enter the type of report, e.g. interim, progress, summary, annual or final. Give the inclusive dates when a specific reporting period is covered). DREA Technical Memorandum		
8. SPONSORING ACTIVITY (the name of the department project office or laboratory sponsoring the research and development. Include address). 		
9a. PROJECT OR GRANT NO. (if appropriate, the applicable research and development project or grant number under which the document was written. Please specify whether project or grant). Project 1gc	9b. CONTRACT NO. (if appropriate, the applicable number under which the document was written). 	
10a. ORIGINATOR'S DOCUMENT NUMBER (the official document number by which the document is identified by the originating activity. This number must be unique to this document.) DREA TM/97/254	10b. OTHER DOCUMENT NOS. (Any other numbers which may be assigned this document either by the originator or by the sponsor.) 	
11. DOCUMENT AVAILABILITY (any limitations on further dissemination of the document, other than those imposed by security classification) <input checked="" type="checkbox"/> Unlimited distribution <input type="checkbox"/> Distribution limited to defence departments and defence contractors; further distribution only as approved <input type="checkbox"/> Distribution limited to defence departments and Canadian defence contractors; further distribution only as approved <input type="checkbox"/> Distribution limited to government departments and agencies; further distribution only as approved <input type="checkbox"/> Distribution limited to defence departments; further distribution only as approved <input type="checkbox"/> Other (please specify):		
12. DOCUMENT ANNOUNCEMENT (any limitation to the bibliographic announcement of this document. This will normally correspond to the Document Availability (11). However, where further distribution (beyond the audience specified in (11) is possible, a wider announcement audience may be selected).		

UNCLASSIFIED

UNCLASSIFIED
SECURITY CLASSIFICATION OF FORM
(highest classification of Title, Abstract, Keywords)

13. **ABSTRACT** (a brief and factual summary of the document. It may also appear elsewhere in the body of the document itself. It is highly desirable that the abstract of classified documents be unclassified. Each paragraph of the abstract shall begin with an indication of the security classification of the information in the paragraph (unless the document itself is unclassified) represented as (S), (C), (R), or (U). It is not necessary to include here abstracts in both official languages unless the text is bilingual).

Ship hulls suffer various types of damage during operation. This damage can be corrosion caused by the marine environment or dents resulting from external forces. In order to make efficient repair decisions, residual strength of the damaged component needs to be assessed. The assessment can be carried out with numerical models such as nonlinear finite element methods or simplified approaches, but this requires experimental verification. DREA conducted a joint stiffened panel strength testing project with the U. S. Interagency Ship Structural Committee (SSC). Five stiffened panels in this project, having dimensions approximately equal to a typical stiffened panel at the upper deck of the Canadian Patrol Frigate (CPF), had deliberately created damage. Three of the panels had part of the web or flange of the stiffener removed while the other two had permanent deflection caused by large lateral forces. A series of finite element analyses were conducted to predict the collapse load as well as to simulate the buckling behaviour. This memorandum summarizes the finite element results and their relation with the test observations. Some discussion and suggestions are also provided.

14. **KEYWORDS, DESCRIPTORS or IDENTIFIERS** (technically meaningful terms or short phrases that characterize a document and could be helpful in cataloguing the document. They should be selected so that no security classification is required. Identifiers, such as equipment model designation, trade name, military project code name, geographic location may also be included. If possible keywords should be selected from a published thesaurus. e.g. Thesaurus of Engineering and Scientific Terms (TEST) and that thesaurus-identified. If it not possible to select indexing terms which are Unclassified, the classification of each should be indicated as with the title).

Stiffened Panel
Nonlinear Finite Element Method
Test Set-up
Residual Stress
Initial Imperfections
Damage
Corrosion

UNCLASSIFIED
SECURITY CLASSIFICATION OF FORM

**D
R
E
A**



**C
R
D
A**